Chapter 5. Single-Electron Spectroscopy

Academic and Research Staff

Professor Raymond C. Ashoori, Dr. Stuart Tessmer, Dr. Nikolai Zhitenev

Graduate Students

David B. Berman, Mikhail G. Brodsky, Ho Bun Chan, Paul I. Glicofridis

Undergraduate Students

Eralp Atmaca, Omar A. Saleh

5.1 Introduction

We have extended our ultra-sensitive capacitance measurements to investigate several systems to which it is not feasible or desirable to make direct electrical contact. Specialized field-effect transistors (FETs) and single-electron transistors (SETs) sense electrical charge inside the semiconductor with noise levels from 10^{-2} to as a low as 10^{-5} electrons $/\sqrt{H}$ z, and the motion of single electrons far beneath the surface can be readily detected. The experimental data provide a new window on the physics *inside* materials in two key ways. First, we study *single* isolated impurities and quantum dots in a *spectroscopic* fashion. Second, we scan the charge sensors to provide these results with high spatial resolution. We also use the scanned measurements to determine the local conductivity in regions underneath the surface.

5.2 Scanning Probe Microscopy to Look Beneath the Surfaces of Samples

Sponsors

### 5.2.1 Scanning Capacitance Microscopy of the Quantum Hall Effect

Project Staff

Dr. Stuart Tessmer, Professor Raymond C. Ashoori

Since the discovery of the quantum-Hall effect in 1980, physicists have drawn schematic pictures to illustrate hypothetical structure of the two-dimensional electron gas (2DEG) in the presence of a quantizing magnetic field. We have recently developed a technique which permits direct imaging of this structure with ~ 300 Å resolution. We constructed a scanning tunneling microscope that is designed to work both in the usual tunneling mode and a novel capacitance mode. The microscope operates in a liquid helium-3 cryostat at 300 mK equipped with a magnet permitting application of fields up to 12 Tesla.

An insulating AlGaAs (~1000 Å thick) layer separates the 2DEG from the sample surface. The initial approach to the sample is achieved in tunneling mode with a sufficiently large applied bias between the tip and the 2DEG to permit electron tunneling through the AlGaAs layer. With the surface found, the microscope is switched into capacitance mode. The tip is scanned at fixed height (typically 50 Å) above the sample surface. We tune two different parameters: tip bias and magnetic field strength. A simplified diagram of this setup is shown in figure 1.
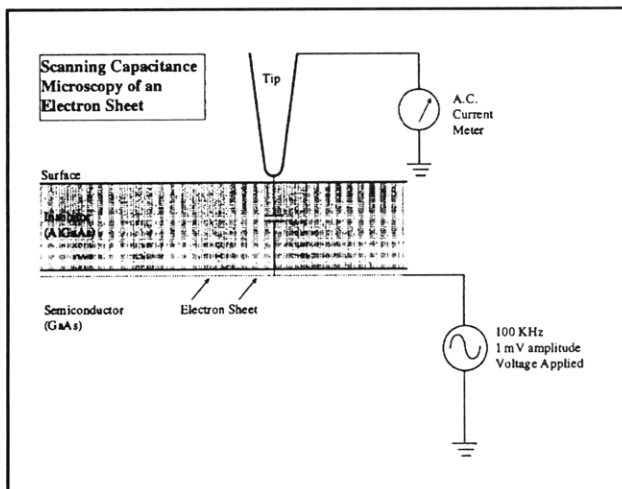
Figure 1. Basic schematic for the low temperature scanning capacitance measurement.

Figure 2.

Figure 2 displays results from our early data runs study 2DEG samples at low temperatures. Figures 2a and 2b are topographic images taken by applying a large positive voltage (4 volts) to the STM tip and monitoring the tunneling current to a 2DEG 1000 Å below an insulating AlGaAs surface. Notice that the surface of these MBE grown wafers is not perfectly flat! Figure 2a was taken on a sample with approximately 2 microns of total epitaxially grown material, whereas 2b was taken on a surface with less than 1 micron of total growth. The bulbous formations on figure 2a arise from Gallium island formation during MBE growth. As might be expected, this effect is diminished when the total growth thickness is reduced (as in figure 2b). With the surface found, the microscope is switched into capacitance mode. The tip is scanned at fixed height (typically 50 Å) above the sample surface. We tune two different parameters: tip bias and magnetic field strength. The capacitance signal is measured with a 1 mV amplitude 100 KHz excitation on the 2DEG.

Regions of the 2DEG which are near integer Landau level filling fraction in filling appear black in the figures. This arises because charge cannot readily flow into or out of these "incompressible" regions. Other, "compressible" regions display varying brightness according to their conductivities. This behavior is clearly seen in figure 2c, taken in a magnetic field of 4 Tesla, where a black region of incompressible fluid appears at the center of the image. The boundaries between these regions vary substantially in position as the magnetic field strength is changed, and the shapes of these boundaries are significantly different than simple models would suggest. This direct imaging of a
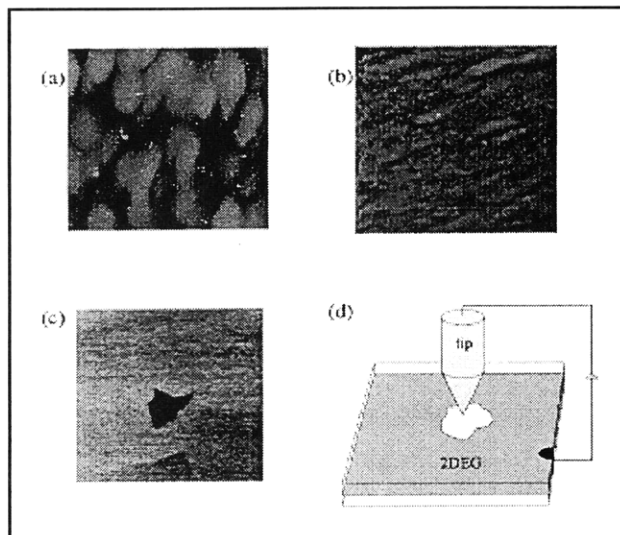
quantum fluid reveals a fascinatingly complex sea of distinct phases.

Significant further experimentation is possible. For instance, we can lower the density underneath the tip by applying a negative voltage to the tip. The result of this is depicted in figure 2d. In zero magnetic field, moving the hole and measuring the scanned capacitance us about density fluctuations within the two-dimensional electron gas. As the tip moves the hole around, the size and shape of the hole changes due to local density variations. Therefore the capacitance between the tip and the 2DEG therefore changes as the tip is moved, and a rough map of the spatial fluctuations in the 2DEG density is thereby obtained.

Clearly, there are a number of profound implications for this new microscope. The next series of experiments will focus on direct observation of single electrons moving into single traps. This experiment will be carried out on GaAs samples much like those used for the SECS experiments on quantum dots discussed above. The sizes and shapes of these traps can be directly examined as well as their spatial distribution. The microscope has many practical implications as well. It is a powerful tool for examination of charge densities which lie underneath the sample surface. Lateral doping profiles can be quickly obtained from local C-V measurements using this new probe. Additionally, single defects and traps in the Si-SiO2 system can be observed directly. Bulk C-V measurements which have been performed for many years can now be taken in a spatially resolved fashion with hugely increased sensitivity.

5.3 Single-Electron Capacitance Spectroscopy: Study of Quantum Dots

Sponsors

Project Staff

David B. Berman, Professor Raymond C. Ashoori, Professor Henry I. Smith

SECS has become a powerful tool for studying quantum dots. Figure 3a shows schematically the type of sample used in one of our SECS experiments. The quantum dot is located between two capacitor plates. It is close enough to one of the plates to allow single electrons to tunnel between the dot and the nearby plate. The dot is far enough from the other capacitor plate to prohibit tunneling to this plate.

How is such a sample actually realized? First, we start with a GaAs/AlGaAs heterostructure grown by molecular-beam epitaxy. The heterostructure contains a 150 Å-wide quantum well which is separated from a metallic substrate by a thin (100 Å) tunnel barrier. By placing electrostatic gates on the surface of the wafer, we can laterally confine electrons in the quantum well and thereby create a quantum dot.

Figure 3b demonstrates how the schematic picture shown in figure 1a is realized in an experiment. A crystal wafer is grown layer by layer, starting from the bottom of the diagram. The first layer is a silicon doped GaAs layer. The silicon doping makes this layer metallic, and it acts as the bottom capacitor plate of figure 3a. Then a thin AlGaAs barrier layer is grown. This barrier is thin enough that electrons can leak through it. Above that, there is a GaAs quantum well, and grown on top of the well is a thick (not leaky) AlGaAs barrier. On top of the crystal wafer, chrome metal is evaporated to form the top capacitor plate, which I will refer to as the "gate." A single 300 Å deep etch on the top surface of the sample is all that is required to laterally confine the electrons into a quantum dot.

Electric fields can be created by applying a voltage between the plates of the capacitor. If the top plate is made positive compared to the bottom one, electrons from the bottom plate will be attracted in the direction of the top plate, toward the artificial atom.
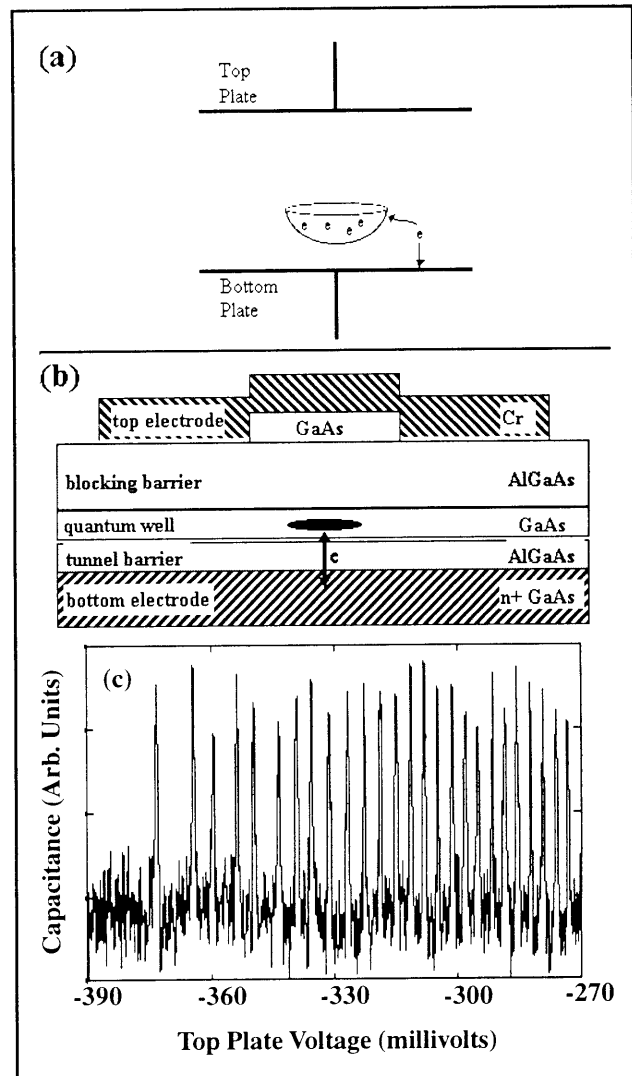
Figure 3. (a) Schematic of the SECS experiment on a single quantum dot. Electrons can tunnel from the bottom plate into the bowl-like potential. (b) Schematic of the quantum dot sample. (c) Spectrum from a SECS measurement on a single quantum save

Single electrons can thus be coaxed to tunnel into the dot or expelled from it through the application of voltages on the top plate.

After each electron is added to the dot, it generally takes additional gate voltage to coax another electron onto the dot. This happens partly because after each electron is added to the dot, other electrons are more strongly repelled from entering the dot. There are, therefore, specific gate voltages at which an electron is added to the dot, and it is this spectrum of voltages (the electron addition spectrum) which has been particularly useful in understanding quantum dots.

The motion of the single electrons into or out of the dot can be detected using a simple physical prin-

ciple. When a single electron tunnels into the artificial atom, it moves closer to the top plate of the capacitor, and electrons in the top plate tend to be pushed away from the plate; i.e., some charge is induced on the top plate. In these samples, the amount of charge induced is about half of an electron's charge. A specialized transistor enables detection of this charge and thereby allows measurement of the gate voltages at which single electrons were added to the artificial atom. A small AC voltage of frequency around 100 KHz is added to the DC gate voltage. When the gate voltage is tuned to a voltage at which an electron can be added to the dot, the AC voltage causes the electron to tunnel back and forth between the dot and the bottom plate. At these gate voltages, charge appears synchronously with the AC voltage. A synchronous detector then registers a signal only at these voltages, yielding a peak in the response. The scheme measures the capacitance signal due to a single electron and is known as single-electron-capacitance spectroscopy (SECS).

Results from this method, taken on a sample cooled to 0.3 Kelvins, are shown in figure 3c. The first peak on the left of the graph corresponds to the *first* electron in the quantum dot. Subsequent peaks correspond to additional electrons added to the quantum dot. The peak structure is completely reproducible as one scans the gate voltage up and down, and the widths of the peaks directly reflect the temperature of the sample.

5.4 A Remarkable New Effect

Sponsors

Project Staff

Ho Bun Chan, Professor Raymond C. Ashoori

In previous measurements, we had noticed a very unusual effect. The Coulomb blockade phenomenon (see section on research in Marc Kastner's group below) is usually dictates that peaks such as those shown in figure 1 are well spaced. This is a simple consequence of more energy being required to add each successive electron to the dot due to repulsion from electrons inside the dot. Very strangely, in some samples we have observed some electron peaks which lie exactly on top of one

another. Somehow the Coulomb blockade effect is not operative in these samples. This phenomenon has been referred to as "negative-U" or an effective negative Coulomb energy for adding electrons to the dot. Two papers have been written suggesting possible explanations for our observations. The origin of the effect has remained controversial, largely because negative-U explanations suggests that the pairs of electrons should display sharply reduced rates for electron tunneling into and out of the dot. This reduced tunneling rate is not observed.

The strange pairing phenomenon was first observed in samples containing large (1 micron diameter) quantum dots. These samples are in a sense not really quantum dots. Instead, the first electrons which enter these samples reside in random potential minima of an impurity potential. Nonetheless, it was very surprising that many pairs of electron peaks (in SECS spectra such as those seen in figure 3c) were observed.

Small dots (which could be considered as true quantum dots and with a lithographic diameter of around 0.2 microns) did not display the pairing phenomenon. We took this as a hint that the observed pairs might actually arise from electrons entering separate random potential minima, but some physical process was making electrons enter the separate minima at precisely the same gate voltages.

We decided to perform careful study of different size quantum dots to determine the origin of the pairing effect. We found that the pairing effect persists in dots of 0.4 microns or larger. However the effect appears in a rather different guise in small dots. The spectra for the first few electrons entering these dots may appear much like those for smaller dots. Features clearly associated with few electron effects can be seen in these dots. For example, a singlet-triplet crossing is observed in the two electron dot. Strangely, however, though the first electron peaks may be well separated, higher in the spectra one observes two electrons and sometimes even three entering the dot at a particular value of the gate voltage. As far as we have been able to ascertain, the bunching effect in the spectra occurs nearly at random. It does not appear possible to predict which peaks in a spectrum will be bunched.

At some point, as one adds more electrons to the dot, it becomes reasonable to think of the dot as a metallic island. Indeed, the SECS spectrum becomes periodic in for large electron numbers (N > 50) just as it was in the smallest dots. However, a fascinating behavior develops.

Applying magnetic field perpendicular to the plane of the quantum dot alters the observed spectra
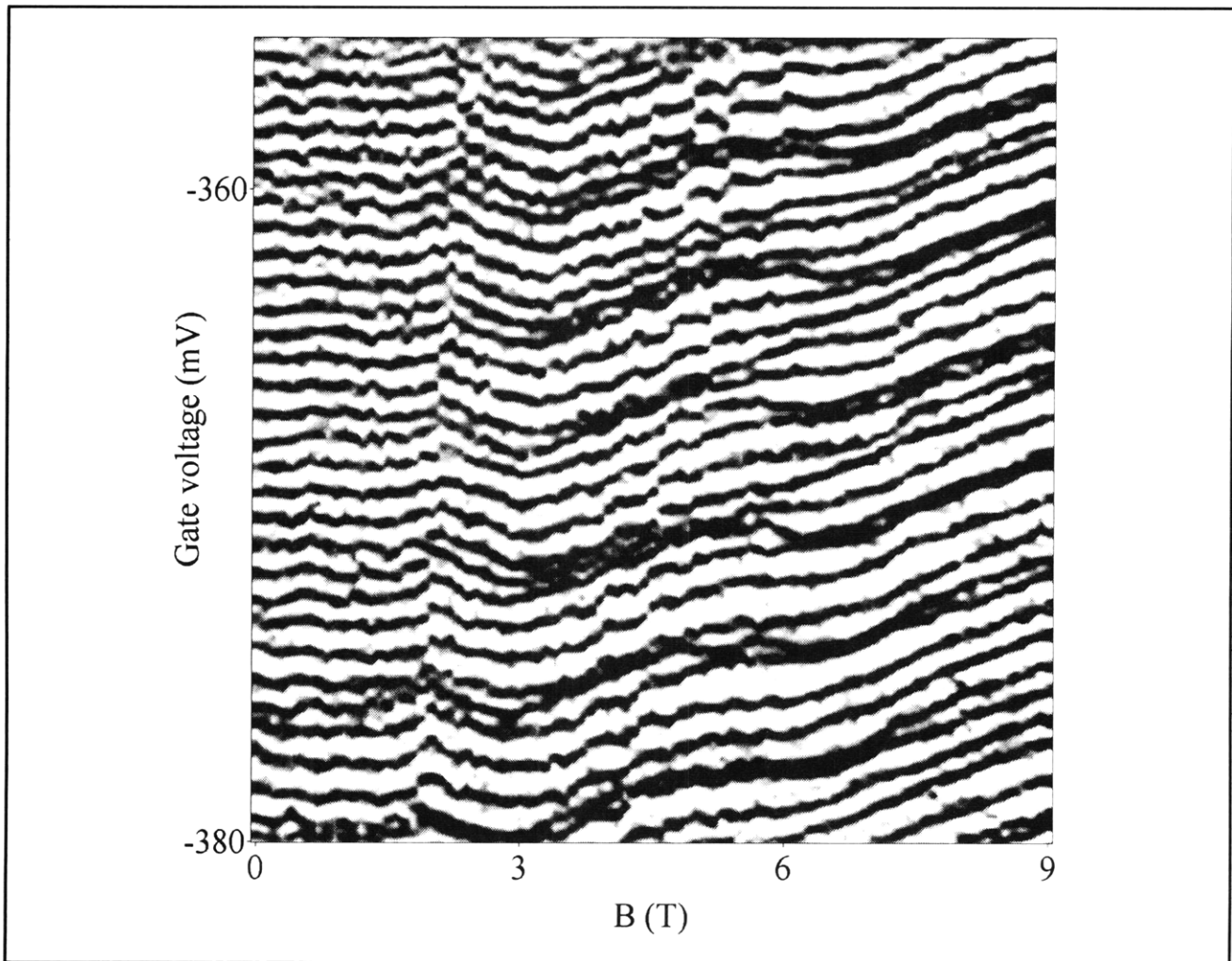
Figure 4.

(some particular characteristics of this alteration are described in the section on professor Marc Kastner's research below). In our intermediate size quantum dots, magnetic field causes the bunching effect seen at low electron numbers to reappear! However, the bunching effect takes a much more ordered appearance. For broad regions of the spectra, every fourth or fifth electron peak is paired.

Figure 4 displays a grayscale capacitance image produced from SECS data. The figure is generated from capacitance versus gate bias scans (similar to those of figure 3c) for a 0.5 mm diameter sample. A sequence of 100 scans, at stepped magnetic field values, is compiled to form this raster image. The dark traces represent capacitance peaks. Higher gate voltages appear higher up on this figure. At the bottom of the figure is the trace for the 71st electron to enter the dot, and at the top is the 101st electron trace.

Notice that at zero magnetic field, the capacitance peak traces appear very nearly periodically as a function of gate voltage. Interestingly, as the magnetic field is increased, the spacings between traces become uneven until finally some traces are seen to form pairs. This behavior appears to be a universal phenomenon. We have observed it in all dots studied with sizes lithographic diameters ranging from 0.4 to 0.8 microns. A distinct magnetic field can be identified for the onset of the pairing effect. The magnetic field strength required for producing the pairing increases as the number of electrons in the dot is increased.

A close study of figure 4 reveals a feature which we feel gives a critical hint as to the origin of the pairing phenomenon. A broad bump in each of the traces at around 3 Tesla demarcates the magnetic field at which all of the electrons in the dot fall into the lowest Landau level. Moving slightly towards higher fields, the electrons in the dot start to spin polarize. In fact, kink like features appear in each

electron trace resulting from spin-flipping events. These kinks are also observed in the paired traces. As the magnetic field is increased to around 7 Tesla, the paired traces break-up. Moving to even higher fields, it is becomes clear that one of the traces from the pair has abandoned its partner to instead pair up with the trace below it! Moreover, the field at which this break-up happens is precisely the same field at which the kinks in the traces cease and the electrons in the dot are thought to be completely spin polarized.

While we do not yet have a complete picture for the origin of the pairing phenomenon, several theoretical ideas have been proposed for the observed behavior. First and foremost, the data strongly suggest that the pairing effect arises as an effect of electron localization into distinct regions of the quantum dot. The pairing simply does not occur in the smallest dots. In the few electron limit, pairs are observed because electrons enter separated sites that somehow "communicate" with each other. Because the puddles are separate, the Coulomb energy cost for adding electrons to isolated sites may not actually be as severe as at first thought. Leonid Levitov is developing a model to describe how pairing develops when isolated "puddles" of electrons merge as more electrons are added to the quantum dot system. Second, the fact that the pairing phenomenon redevelops, as the magnetic is increased, is consistent with the notion that magnetic fields may cause electrons in the dot to break up into isolated annular regions. Electrons are effectively localized into separate regions of an annular dot and are separated enough that the Coulomb interaction does not prohibit pairing. Third, the fact that the pairing breaks down at fields which are thought to polarize the electron spins in the dot suggests that a kind of effectively attractive antiferromagnetic exchange interaction is responsible for the effect.

The results shown in figure 4 are highly repeatable and occur in a wide variety of dots. They have not been seen in other experiments on semiconductor quantum dots. We believe that the chief reason for this is that our experiments can monitor the regime of localized electrons in a quantum dots. Most transport experiments demonstrate electron charging by passing current through a dot. If the dot is broken up into isolated islands, the transport experiments simply show no signal. Moreover, if the dot breaks up into annular regions as we

suspect, transport experiments might only develop observable signals from electrons entering the outer shell of the dot.

Our experiments are the first performed on quantum dots that show a clear transition between localized and delocalized regime. The insulator to metal transition can be studied in a profound new way, and these measurements have led to a very surprising result.

5.5 Tunneling into Two-Dimensional Systems

Sponsors

Project Staff

Dr. Nikolai Zhitenev, Mikhail G. Brodsky, Professor Raymond C. Ashoori

We have developed a new technique which permits high-fidelity measurement of the tunneling density of states of the two-dimensional electron gas. This method allows us to obtain the complete I-V characteristics of structures to which direct ohmic contact is not possible. The tunneling current into a 2D electron system can now be measured at arbitrarily low values of in-plane conductivity, a regime of great theoretical interest but experimentally difficult to access.

Figure 5a depicts the type of samples used in our experiment. Our sample is a GaAs/AlGaAs heterostructure grown by molecular beam epitaxy. The 2D electron system is sandwiched between two electrodes, close enough only to the bottom electrode to permit tunneling of electrons. Figure 5b shows the evolution of the conduction band diagram for our samples during one cycle of measurement. We start with the 2D electron system in equilibrium with the 3D substrate. At time t = 0, a sharp voltage step is applied. This creates an offset in the chemical potential on the two sides of the tunnel barrier, inducing a tunneling current. As electrons tunnel, this offset equilibrates, and the decay signal is recorded in real time.
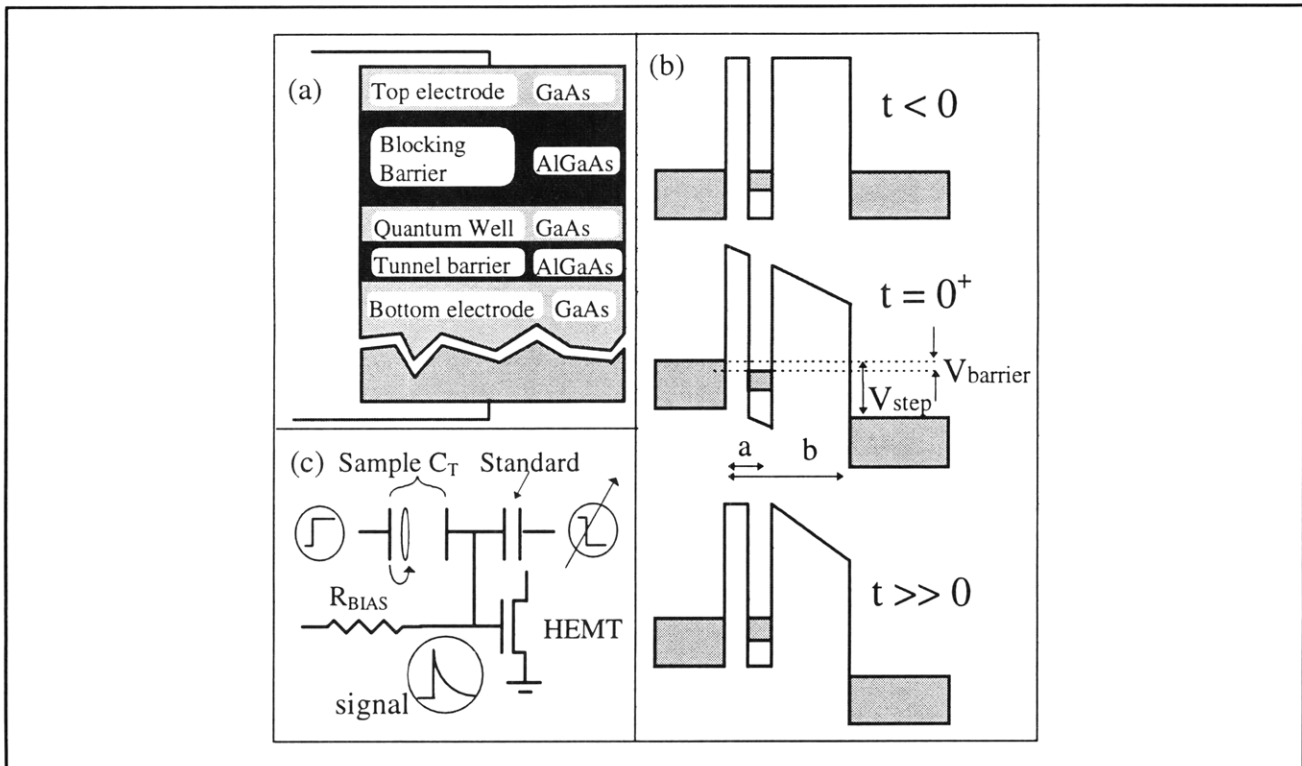
Figure 5.

Before the voltage step is applied, the 2D plane has the same electrochemical potential at all positions. Immediately after the voltage step is applied (t = 0+), no charge has been transferred into the 2D electron system. The voltage pulse is not screened by the quantum well and the 2D plane remains an equipotential. The simple planar geometry of the sample dictates that this remains true even in situations of very low 2D conductivity. At t = 0+, the voltage across the tunnel barrier ($V_{barrier}$) is simply a fraction of the voltage step applied (V_{step}), given by $V_{barrier} = a/bV_{step}$ with a and b defined in figure 5b. The 3D substrate is always highly conducting, and electrons can tunnel everywhere into the 2D electron system.   Using charge conservation we have determined that immediately after the applied voltage step, the current across the barrier is found to be proportional to the initial time derivative of the voltage at the balance point. By applying voltage steps of different amplitude and taking initial time derivatives of the corresponding transistor signal, the complete I-V characteristics of the tunnel barrier can be mapped out.

Figure 6 shows the tunneling conductance (I/V) plotted against the voltage across the barrier for magnetic field strengths of 0, 1, 2, 8 and 16 Tesla

at a fixed electron density of 1.9×10^{11} cm^{-2} . In the absence of a magnetic field, there is no anomaly in the conductance. Application of a magnetic field reduces the tunneling conductance around zero bias. The suppression becomes deeper and wider as the field is increased. Moreover, an increase in the strength of the suppression is accompanied by a change in the curvature of the high excitation part of the conductance curves when the magnetic field is increased, as shown by the bottom inset of figure 6. Even though the conductance curves at high excitation appear rounded at high fields, the zero bias region remarkably remains linear in voltage, with both the magnitude and the slope significantly reduced. Such a linear energy dependence of the TDOS is observed over the full range of densities except near depletion. Moreover, the slope of this linear gap is found to be strongly field dependent. We have proposed a phenomenological model to explain this observation.

The top left inset of figure 6 displays a conductance curve from sample B at a field of 4T and ν ~3. In addition to the zero bias suppression, features associated with adjacent Landau levels can be identified at higher excitations.
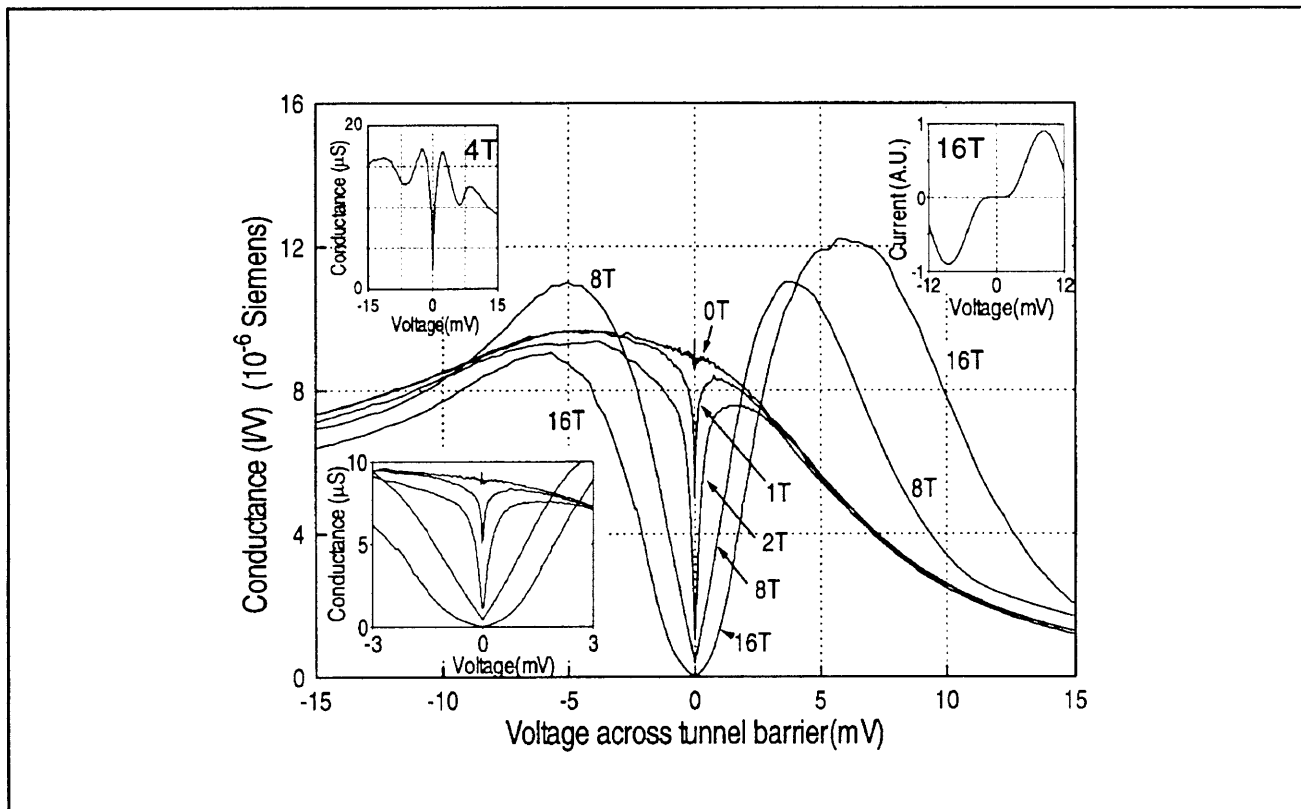
Figure 6.

5.6 Publications

Ashoori, R.C. "Electrons in Artificial Atoms." *Nature* 379: 413-419 (1996).

Chan, H.B., R.C. Ashoori, and M.R. Melloch. "Universal Linear Density of States for Tunneling into the Two-Dimensional Electron Gas in Magnetic Field." Submitted to *Phys. Rev. Lett.*

Tessmer, S.H., R.C. Ashoori, and M.R. Melloch. "Scanning Capacitance Microscopy of the Quantum Hall Effect." In preparation for submission to *Sci.*

Zhitenev, N.B., M. Brodsky, R.C. Ashoori, and M.R. Melloch. "A New Class of Resonances at the Edge of the Two-Dimensional Electron Gas." *Phys. Rev. Lett* 77: 1833-1836 (1996).

Zhitenev, N.B., R.C. Ashoori, L.N. Pfeiffer, and K.W. West. "Periodic and Aperiodic Bunching in the Addition Spectra of Quantum Dots." Submitted to *Phys. Rev. Lett.*